

# Solar modulation of cosmic proton and helium with AMS-02

Bing-Bing Wang<sup>1,2</sup>, Xiao-Jun Bi<sup>3,4</sup>, Kun Fang<sup>3</sup>, Sujie Lin<sup>5</sup>, and  
Peng-Fei Yin<sup>3</sup>

<sup>1</sup>Department of Space Science, University of Alabama in Huntsville,  
Huntsville, AL 35899, USA

<sup>2</sup>Center for Space Plasma and Aeronomic Research (CSPAR),  
University of Alabama in Huntsville, Huntsville, AL 35899, USA

<sup>3</sup>Key Laboratory of Particle Astrophysics, Institute of High Energy  
Physics, Chinese Academy of Sciences, Beijing 100049, China

<sup>4</sup>School of Physical Sciences, University of Chinese Academy of  
Sciences, Beijing 100049, China

<sup>5</sup>School of Physics and Astronomy, Sun Yat-Sen University, Zhuhai  
519082, GuangDong, China

November 26, 2020

## Abstract

We investigate the solar modulation effect with the long time cosmic ray proton and helium spectrum measured by AMS-02 on the time scale of a Bartels rotation (27 days) between May 2011 and May 2017. The time-span covers the negative heliospheric magnetic field polarity cycle, the polarity reversal period and the positive polarity cycle. The unprecedented accuracy of AMS-02 observation data provide a good opportunity to improve the understanding of the time dependent solar modulation effect. In this work, a two-dimensional solar modulation model is used to compute the propagation of cosmic rays in the heliosphere. Some important ingredients of the model which reflect the global heliospherical environment are taken from the observations. The propagation equation is numerically solved with the public Solarprop code. We find that the drift effect is suppressed during the high solar activity period but nearly recovered in the first half of 2017. The time-dependent rigidity dependence of the mean free path is critical to reproduce the observations between August 2012 and October 2015.

We also confirm that the proton and helium have the same diffusive mean free path. The future monthly AMS-02 and PAMELA data will further confirm the vital assumption on the universal mean free path for all species; the antiproton data will be crucial to determine the drift effect during different epochs.

## 1 Introduction

The galactic cosmic rays are believed mainly come from supernova remnants. After injected from the sources, cosmic rays propagate in the interstellar space. When cosmic rays enter the heliosphere, the interaction with the solar wind and the embedded magnetic field results in the intensity and the spectral shape of low energy cosmic rays are different from the local interstellar spectrum (LIS) [1, 2]. These effects on cosmic rays are called solar modulation. The solar modulation effect limits our understanding for cosmic rays outside the heliosphere. Therefore, the study of solar modulation is important for studying the injection and propagation parameters of cosmic rays, dark matter indirect measurement and the diffusion theory in the galaxy and heliosphere [3, 4, 5, 6, 7, 8, 9, 10, 11, 12, 13, 14, 15, 16].

The recent experimental results from Voyager 1, PAMELA, and AMS-02 have achieved great breakthroughs which are useful to understand the solar modulation effect. The Voyager 1 flew outside the heliosphere on August 2012 and directly measured the LIS in the range from a few to hundreds MeV/nucleon [17, 18, 19]. The monthly PAMELA measurements of proton spectra [20, 21] shed light on some details of the solar modulation [22, 23, 24, 25, 26, 27, 31]. Recently, the AMS-02 collaboration has published the continuous proton and helium energy spectrum with rigidity above 1 GV for proton and 1.9 GV for helium between May 2011 and May 2017 [28]. Some important results have been obtained, such as the confirmation of the velocity dependence of cosmic ray diffusion and finding the increase of the slope of perpendicular mean free path during solar maximum for low rigidity particles [29, 30].

In [31] (hereafter Paper I), we build a modulation model to well reproduce the long time PAMELA proton measurements between July 2006 to February 2014. This modulation model includes mainly physical processes affecting the propagation of cosmic rays in the heliosphere: diffusion, convection, drift, and energy loss. Meanwhile, some main factors affecting solar modulation are taken from observations, such as the magnitude of the heliospheric magnetic field, the solar wind speed, and the tilt angle of the heliospheric current sheet (HCS). We adopt the same model in this work.

We also deliberate to keep the model as simple as possible by only including the minimal degree of freedom. The 2D modulation code `solarprop`<sup>1</sup>[32] is used to solve the cosmic ray propagation equation and obtain the modulated spectra. In Paper I, we find that the modulation processes are different between negative and polarity reversal period. Therefore, we analyze the modulation effect with AMS-02 proton data separately in three periods related to the magnetic field polarity. After successfully reproducing the proton observations, the modulation parameters for proton are applied to calculate the modulated helium spectrum.

The paper is organized as follows. In Section 2, we briefly introduce the modulation model and present the LIS for proton and helium. In Section 3, we compute the modulated proton spectrum and compare them to observations. In Section 4, we check the assumption that proton and helium have the same mean free path by computing the helium spectrum with the modulation parameters for proton. Finally, we give a summary in Section 5.

## 2 A 2D solar modulation model

There are four major modulation mechanisms for cosmic rays in the heliosphere: diffusion on irregularities of the heliospheric magnetic field, convection by the outward solar wind, particles drift in the non-uniform magnetic field and adiabatic energy loss. Several review articles discuss the modulation process in great detail [1, 2]. The propagation process can be described by the Parker equation [33]:

$$\frac{\partial f}{\partial t} = -(\vec{V}_{sw} + \vec{V}_{drift}) \cdot \nabla f + \nabla \cdot [K^s \cdot \nabla f] + \frac{\nabla \cdot \vec{V}_{sw}}{3} \frac{\partial f}{\partial \ln p}, \quad (1)$$

where  $f(\vec{r}, p, t)$  is the omni-directional distribution function,  $\vec{r}$  is the position in the heliocentric spherical coordinate system,  $p$  is the particle momentum,  $\vec{V}_{sw}$  is the solar wind speed,  $\vec{V}_{drift}$  is the drift speed,  $K^s$  is the symmetric part of diffusion tensor. The differential intensity related with the distribution function is given by  $I = p^2 f$ .

It is customary to assume that the diffusion coefficient can be separated into spatial and rigidity components [2]. The generally assumption about the rigidity part is that all particle species have a universal function of rigidity [34, 35, 36, 37, 38, 39]. In Paper I, we adopt a linear rigidity dependence

---

<sup>1</sup><http://www.th.physik.uni-bonn.de/nilles/people/kappl/>

of the diffusion coefficient and can reproduce the PAMELA monthly proton measurements between 2006 to 2012. But during the polarity reversal period which is assumed between November 2012 and March 2014 in Paper I based on Ref. [52], the time-dependent rigidity dependence is necessary to reproduce the observations. In the present work, the parallel diffusion coefficient is adopted as the following form taking into account the finding in Paper I:

$$k_{\parallel} = \frac{1}{3}k\beta\left(\frac{R}{1\text{ GV}}\right)^{\delta}\frac{B_E}{B} \quad (2)$$

where  $k = 3.6 \times 10^{22}k_0 \text{ cm}^2/\text{s}$  is a scale factor to model the time dependence of the diffusion coefficient,  $\beta$  is the particle speed in the unit of the speed of light,  $\delta$  determines the rigidity dependence of the diffusion coefficient (by default  $\delta = 1$ ),  $B_E$  is the heliospheric magnetic field strength near the Earth,  $B = B_0/r^2\sqrt{1 + \tan^2\psi}$  is the heliospheric magnetic field strength at the particle position and  $\psi$  is the angle between magnetic field direction and its radial direction [40]. The standard Parker magnetic field model [40] is used in this work. We take the perpendicular diffusion coefficient to be  $k_{\perp} = 0.02k_{\parallel}$  according to the test particle simulation [41]. The diffusion coefficient is also often marked as  $k_{\parallel/\perp} = \frac{1}{3}v\lambda_{\parallel/\perp}$ , where  $v$  is particle speed and  $\lambda_{\parallel}$  ( $\lambda_{\perp}$ ) is called the parallel (perpendicular) mean free path.

The gradient and curvature drift speed is written as  $V_{gc} = q\frac{\beta R}{3}\nabla \times \frac{\vec{B}}{B^2}$  [42]. We describe the heliospherical current sheet (HCS) drift following Ref. [43], where a thick, symmetric transition region determined by the tilt angle is used to simulate a wavy neutral sheet. The HCS drift speed  $V_{ns}^w$  is given by

$$\vec{V}_{ns}^w = \begin{cases} qA\frac{v\theta_{\Delta}\cos(\alpha)}{6\sin(\alpha+\theta_{\Delta})}\vec{e}_r, & \pi/2 - \alpha - \theta_{\Delta} < \theta < \pi/2 + \alpha + \theta_{\Delta} \\ 0, & \text{else} \end{cases} \quad (3)$$

where  $q$  is the charge sign and  $v$  is the particle speed,  $\theta_{\Delta} \approx \frac{2RV_{sw}}{B_0\Omega\cos\alpha}$ . When the polar solar magnetic field directs outward in the north (southern) hemisphere and inward in the southern (north) hemisphere, it is said that the Sun is in a positive (negative) polarity cycle marked as  $A > 0$  ( $A < 0$ ).  $qA$  determines the drift direction. Taking into account the possible suppression of the drift effect, a scale factor  $k_d$  (by default  $k_d = 1$ ) is introduced and the drift velocity is described as  $V_{drift} = k_d(V_{gc} + V_{ns}^w)$  [44, 45].

The solar wind speed and the magnitude of magnetic field are taken from the website [omniweb.gsfc.nasa.gov](http://omniweb.gsfc.nasa.gov). The tilt angle of HCS is obtained from the website [wso.stanford.edu](http://wso.stanford.edu) with the “new” model. These quantities

are averaged over several months which corresponds to the time of solar wind propagation from the Sun to the modulation boundary at 100 AU. More elaborate description to our model is given in Paper I and references therein. The discussion about the modulation resulted from the merged interaction regions [46, 47, 48] is not included in the recent work.

As an initial input condition in the modulation model, the LIS are constrained by the current experimental measurements. Voyager 1 has directly measured the LIS in the range from a few to hundreds of MeV/nucleon. The monthly precise AMS-02 data provide important ingredients to reconstruct the LIS. The LIS for proton and helium are constructed by the cubic spline interpolation method following the works [7, 31, 49]. This method avoids the bias comes from the cosmic ray injection and propagation model which is still in debate. We determine the proton and helium LIS by matching the low energy LIS to the Voyager 1 measurements and fitting the calculated spectrum to the AMS-02 data observed during Bartels rotation 2429, 2432, 2435 and 2438 [19, 28]. These time periods are all within the negative polarity and the data can be well explained with one free parameter  $k_0$ . The GNU Scientific Library (GSL)<sup>2</sup> is used to perform the least-squares fitting. The energy knots and the corresponding intensities in the cubic spline interpolation method are shown in Table 1 and 2. The difference between the LIS obtained by this work and that derived in Paper I is very small (see Appendix A). Once the LIS have been derived, the effects of solar modulation are calculated directly from the model.

Table 1: The parameterization of proton LIS with the cubic spline interpolation method.  $E_k$  is kinetic energy and  $I$  is intensity.

$\log(E_k/\text{GeV})$	-2.42	-1.41	-0.50	0	0.50	1.00	1.50	2.00
$\log(I/(\text{GeVm}^2\text{sr s}))$	4.2905	4.4688	4.0176	3.4548	2.5849	1.4158	0.0597	-1.3497

Table 2: The parameterization of helium LIS with the cubic spline interpolation method.  $E_k$  is kinetic energy and  $I$  is intensity.

$\log(E_k/\text{GeV})$	-2.27	-1.28	-0.30	0.56	1.22	1.78	2.29
$\log(I/(\text{GeVm}^2\text{s sr}))$	2.3812	2.7324	2.6735	1.7705	0.4619	-0.8980	-2.2892

<sup>2</sup><https://www.gnu.org/software/gsl/>

### 3 Solar modulation for proton

The AMS-02 data are taken during different solar activity levels and different magnetic field conditions: the negative polarity cycle, the undefined polarity period around the solar maximum and finally the positive polarity cycle. In Paper I, we show that the diffusion and the drift are both different during the negative and the polarity reversal periods. Thus, we investigate the modulation effect for proton separately in three periods related to the magnetic field polarity.

#### 3.1 Modulation of CR proton with the assumption of the negative polarity

During every solar maximum the polarity of the solar magnetic field and subsequently the heliospherical magnetic field reverses direction. After the polarity reversal took place around 2000 [50], the polarity is negative until the recent reversal. During the negative polarity cycle ( $A < 0$ ), positively charged particles drift into the inner heliosphere along the HCS and out over the poles. Due to the asymmetric solar activity, the reversal of the solar magnetic field polarity is not simultaneous in two hemispheres. The summary of some estimates of the solar polar field reversal times for the northern and southern solar hemisphere is presented in Table 3. One can

Table 3: Estimates of the time of solar polar magnetic field polarity reversals in the northern and southern hemisphere.

North	South	Ref.
2012/06	-	[51]
2012/11	2014/03	[52]
2013/07	2015/01	[53]
2012/05-2014/04	2013/06-2015/03	[54]
2012/10-2015/09	2014/06	[55]
2012/06-2014/11	2013/10	[56]

see from Table 3 that the estimated reversal time can be very different by means of different methods and data. The polarity reversal period is not well determined. However, we also see that the polarity reversal process had not happened before the early of 2012. Thus, it is safe to set the heliospheric magnetic field polarity as negative in this time period.

We compare the computed spectrum with the AMS-02 measurements with rigidity below 40 GV. For the particle with higher rigidity, the modu-

lation effect is negligible. Following the scenario in Paper I which reproduces 6 years PAMELA proton spectrum between 2006 to 2012, we fixed both  $k_d$  and  $\delta$  as 1 and only adjust  $k_0$  to fit the observation. The resulting time profile of the reduced- $\chi^2$  ( $\chi^2/(d.o.f.)$ ) is shown in Figure 1. The reduced- $\chi^2$  is around or less than 1 until August 2012. There is no significant need to introduce more free parameter for this period. However, after the August 2012, the reduced- $\chi^2$  suddenly increases to an unacceptable level with reduced- $\chi^2 > 2$ . The model with only one free parameter  $k_0$  fails to correctly describe the modulation process after this time node.

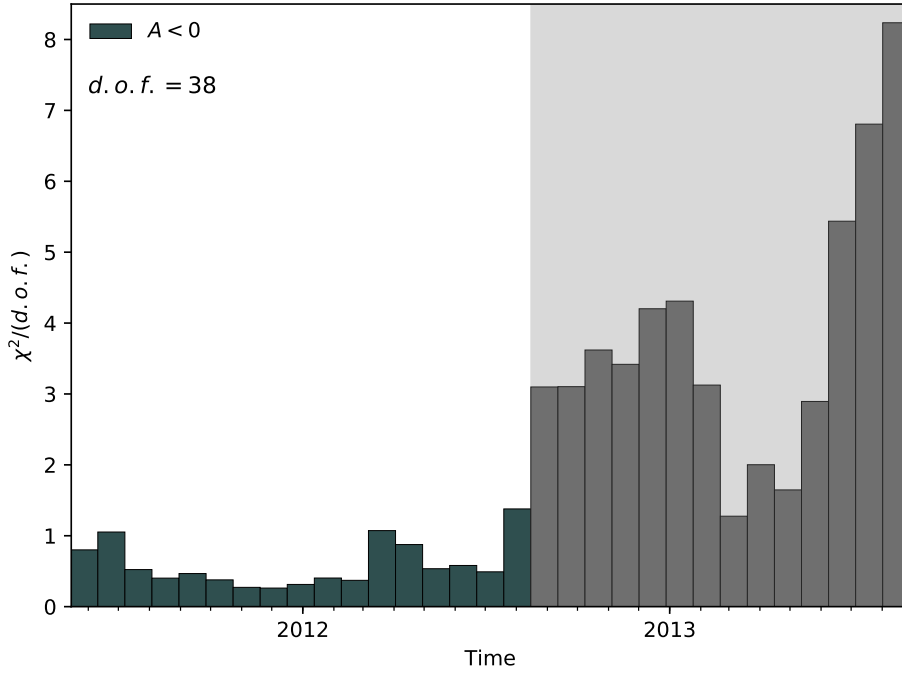


Figure 1: The time profile of reduced- $\chi^2$  for the fit to the monthly AMS-02 proton data between May 2011 and November 2012 under the assumption  $A < 0$ . The scale factor of diffusion coefficient  $k_0$  is taken as the free parameter.

### 3.2 Modulation of CR proton with the assumption of the positive polarity

As showed in Table 3, the estimated latest time of the completion of the reversal is September 2015. After the reversal, the solar magnetic field polarity becomes positive ( $A > 0$ ). Positively charged particles drift into the inner heliosphere over the poles and out of it along the HCS. They have less difficulty in reaching the Earth and less modulation than that during the negative polarity period.

When the solar activity indicated by the sunspot number decreases to moderate level, we expect the turbulence magnetic properties and the rigidity dependence of the mean free path recover to the similar behavior with  $\delta = 1$  as in the negative polarity cycle. We attempted to adopt the full drift effect ( $k_d = 1$ ), but the required scale factor of diffusion coefficient  $k_0$  is much smaller than 0.7 prior to October 2016 (see Appendix B). Under the simple framework of the force-field approximation, the modulation potential is inversely proportional to the diffusion coefficient characterized by  $k_0$ . The ratio of solar modulation potential (also the diffusion coefficient) reconstructed from the neutron monitor count rate [57, 58] is within 2.1 during May 2011 to May 2017. If the full drift effect is adopted, the required diffusion coefficient is too small and far from this relation. In addition, this scenario results in larger  $\chi^2$  than the suppressed drift case (see Appendix B). Thus, we set  $k_d$  as a free parameter in this time period to reduce the drift effect.

In Figure 2 we show that the time profile of reduced- $\chi^2$  and the scale factor for the drift speed  $k_d$ . The reduced- $\chi^2$  values are less than or close to 1 during November 2015 to May 2017. The scale factor of drift velocity  $k_d$  is nearly 0 around the second half of 2015, and it is about 0.8 in March 2017. It indicates that the drift effect is suppressed during this period. The increase of  $k_d$  from 0 to 0.8 indicates the gradual recovery of the drift effect and implies that the drift effect may fully recover around the middle of 2017. There are several mechanisms that may cause the suppression of the drift effect. The large-scale fluctuations in the heliospheric magnetic field, such as the interaction regions and the merged interaction regions, fill the heliosphere so that drifts may only occur on a less scale during moderate to high solar activity period [47]. In addition, numerical simulation shows that the presence of scattering can also suppress the drift effect. For an intermediate degree of scattering, the drift velocity is typically suppressed by a larger degree; when the scattering is very strong, there is no large-scale drift motions [59].



Note that there is some degeneracy between  $k_0$  and  $k_d$  as shown in Appendix C. As the drift effect is opposite for particle with opposite charge, a simultaneous fit to the proton and future antiproton spectrum is crucial to reduce the uncertainty and get a better understanding for the drift effect.

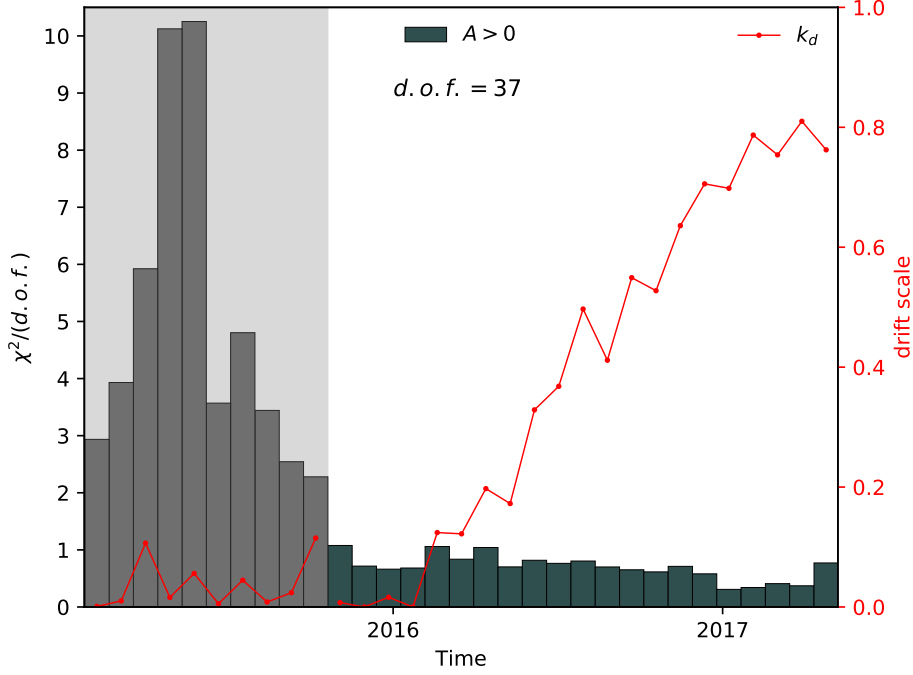


Figure 2: The time profile of reduced- $\chi^2$  and the drift scale factor  $k_d$  from the fits to the AMS-02 proton data during August 2015 to May 2017 under the assumption of  $A > 0$ . The scale factor for diffusion coefficient and drift velocity,  $k_0$  and  $k_d$ , are free parameters in this period.

### 3.3 Modulation for proton between August 2012 and October 2015

From Section 3.1, we show that the default model with the linear rigidity dependence on the mean free path and the full drift effect ( $\delta = 1$ ,  $k_d = 1$ ) fails to describe the modulation process since August 2012. Additionally, the model with linear rigidity dependence on the mean free path and the

suppressed drift effect ( $\delta = 1$ ,  $k_d \in [0, 1]$ ) used in Section 3.2 can not reproduce the observations before October 2015. In Paper I, after we tested various configurations for the diffusion coefficient and drift effect to reproduce the PAMELA proton observations during November 2012 to February 2014, we concluded that the combination of the time-dependent power-law rigidity dependence on the mean free path and the zero drift configuration give the best fit to the data. So in this case, the free parameters are  $k_0$  and  $\delta$ . This scenario is adopted to reproduce the AMS-02 observations between August 2012 and October 2015 which coincides with some estimated polarity reversal periods.

The time profile of the slope of the mean free path  $\delta$  and the reduced- $\chi^2$  are shown in Figure 3. We find that  $\delta$  roughly keeps increasing until it reaches the maximum value of 1.28 in October 2013 and then decreases to 1.07 in October 2015. The variation of rigidity dependence should be noticed in all cosmic ray species, such as helium. Almost all the reduced- $\chi^2$ s are smaller than 1. Obviously, the combination of the two parameters  $k_0$  and  $\delta$  is adequate to reproduce the observations. Although introducing  $k_d$  as the third free parameter may further improve the fit, but the parameter space will not be constrained well because of the degeneracy between diffusion and drift parameters. The future monthly antiproton data is needed to reduce the degeneracy. The drift velocity is assumed to be 0 in this subsection, which may not be realistic in the whole period since it may have a transition process. Because of the degeneracy between the scale factor ( $k_0$ ), the slope ( $\delta$ ) of the diffusion coefficient and the drift speed ( $k_d$ ), these transition processes have to be studied separately in greater detail.

## 4 Solar modulation for helium

It is an important assumption that the mean free path is the same for all species of nuclei. The precise AMS-02 measurements provide a good opportunity to check this widely adopted assumption. The main parameter  $k_0$  for proton is shown in the bottom panel of Figure 4. The time profiles of  $k_d$  and  $\delta$  are shown in Figure 2 and Figure 3, respectively. We take the modulation parameters ( $k_0$ ,  $\delta$ ,  $k_d$ ) obtained in the previous section as inputs to directly compute the modulated spectrum for helium. The reduced- $\chi^2$  for helium and proton are summarized in the upper panel of Figure 4. We find that the same modulation parameters can well reproduce the proton and the helium observations simultaneously. Meanwhile, we show the ratios of the computed intensities to the measured intensities as functions of rigidity

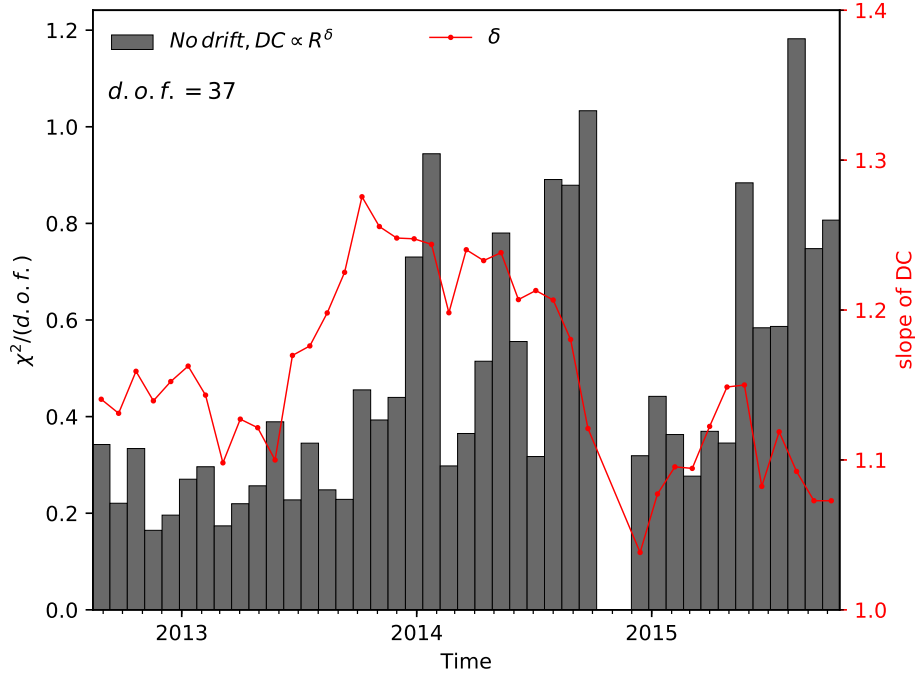


Figure 3: The time profile of reduced- $\chi^2$  and the slope of the mean free path  $\delta$  for the fits to the AMS-02 proton data between August 2012 and October 2015. The scale factor for the diffusion coefficient  $k_0$  and slope for the diffusion coefficient  $\delta$  are free parameters in this period.

and time in Figure 5. It can be seen that most of the fits agree with the data within  $\pm 5\%$ .

Recalling the treatment to the modulation for boron and carbon in Paper I, in which the same mean free paths are able to reproduce the ACE boron and carbon observations, different nuclei could have the same mean free path in the heliosphere. The upcoming monthly helium data of PAMELA between July 2006 and January 2016 [60] and future time-dependent nuclei data of AMS-02 will give it a further test.

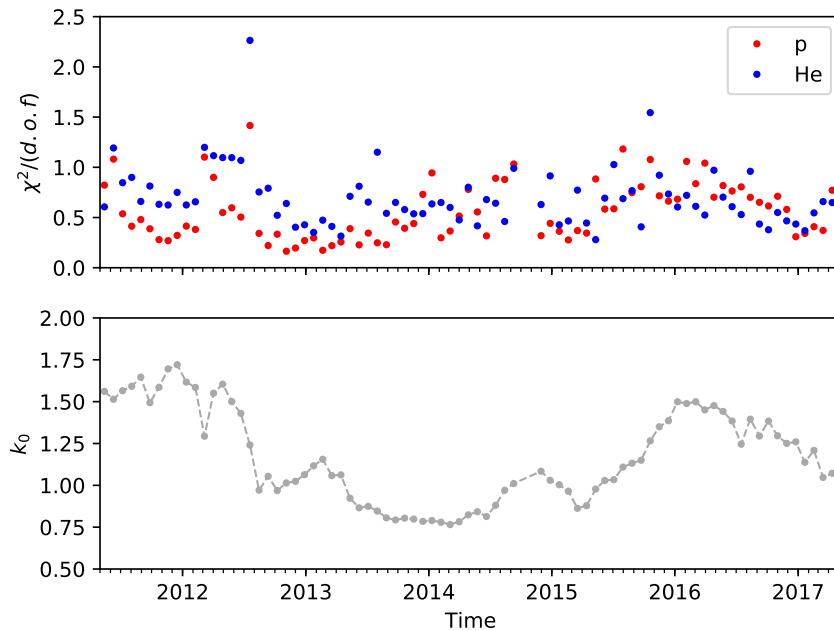


Figure 4: The upper panel shows the time profile of reduced- $\chi^2$  for proton (red dots) and helium (blue dots). The bottom panel shows the best fit  $k_0$  for proton. Note that in the upper panel, the modulation parameters for helium are taken from proton.

## 5 Conclusion

The precise measurements of monthly cosmic ray proton and helium spectra by AMS-02 between May 2011 to May 2017 provide an important chance to improve our understanding for the solar modulation. Compared to the PAMELA data up to February 2014, the AMS-02 data cover the whole solar magnetic field polarity reversal period around the solar maximum and part of the positive polarity cycle. Meanwhile, the precise measurements of monthly helium spectrum provide a chance to check the important assumption that the cosmic ray proton and helium have the same diffusive mean free path in the heliosphere.

A two-dimensional model is used to describe the propagation of proton

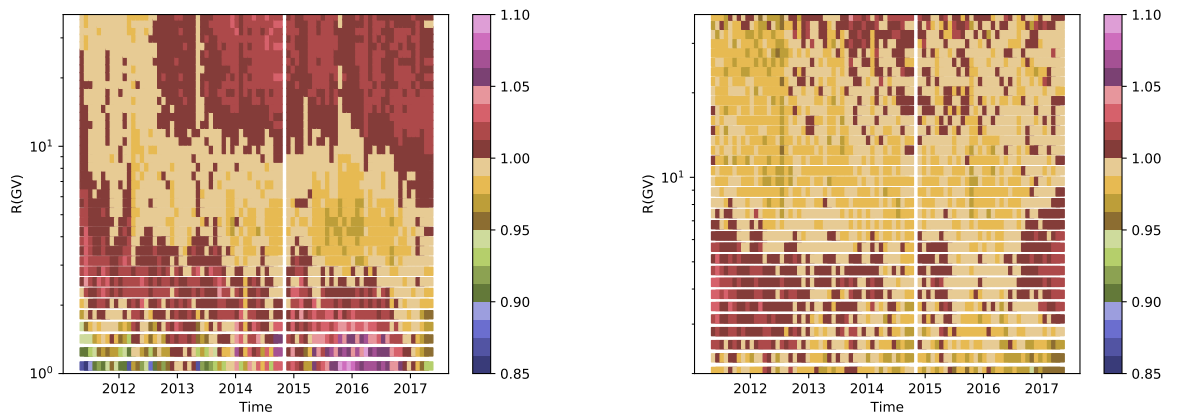


Figure 5: The left (right) panel show the ratio of the computed proton (helium) intensities to measured values. The same modulation parameters are applied for proton and helium.

and helium in the heliosphere. The model includes all major modulation processes and the variation of the heliosphere environment, such as the solar wind speed, the magnetic field strength and the tilt angle of HCS. We consider a simplest reasonable scenario to reproduce the observations. With no more than two free parameters, the computed spectrum are able to match the AMS-02 proton and helium observations.

We find that the rigidity dependence of the mean free path is varied with time. The linear rigidity dependence is adequate to reproduce the observations before August 2012 or after October 2015. Within the possible polarity reversal period between August 2012 and October 2015, the time varying power-law dependence of the mean free path is essential to fit the data. We also find that the zero drift effect can well reproduce the observations during the polarity reversal period and the suppressed drift effect clearly keeps recovering after this period. Finally, with the help of the precise monthly helium measurements, we confirm that the mean free path is the same for proton and helium. The future monthly data from AMS-02 and PAMELA for other nuclei will provide further checking for the assumption that all nuclei have a universal mean free path, and the monthly antiproton data would provide invaluable help to understand the role of the drift effect in different solar activity periods.

## Acknowledgement

This work is supported by the National Key R&D Program of China (No. 2016YFA0400200), the National Natural Science Foundation of China (Nos. U1738209 and 11851303).

## References

- [1] J. R. Jokipii. Propagation of cosmic rays in the solar wind. *Reviews of Geophysics and Space Physics*, 9:27–87, 1971.
- [2] M. S. Potgieter. Solar Modulation of Cosmic Rays. *Living Reviews in Solar Physics*, 10:3, June 2013.
- [3] M. J. Boschini, S. Della Torre, M. Gervasi, D. Grandi, G. Jóhannesson, M. Kachelriess, G. La Vacca, N. Masi, I. V. Moskalenko, E. Orlando, S. S. Ostapchenko, S. Pensotti, T. A. Porter, L. Quadrani, P. G. Rancoita, D. Rozza, and M. Tacconi. Solution of Heliospheric Propagation: Unveiling the Local Interstellar Spectra of Cosmic-ray Species. *ApJ*, 840:115, May 2017.
- [4] Nicola Tomassetti. Solar Modulation of Galactic Cosmic Rays: Physics Challenges for AMS-02. *ArXiv e-prints*, page arXiv:1712.03178, December 2017.
- [5] M. J. Boschini, S. Della Torre, M. Gervasi, D. Grandi, G. Jóhannesson, G. La Vacca, N. Masi, I. V. Moskalenko, S. Pensotti, T. A. Porter, L. Quadrani, P. G. Rancoita, D. Rozza, and M. Tacconi. Deciphering the Local Interstellar Spectra of Primary Cosmic-Ray Species with HELMOD. *ApJ*, 858:61, May 2018.
- [6] M. J. Boschini, S. Della Torre, M. Gervasi, D. Grandi, G. Jóhannesson, G. La Vacca, N. Masi, I. V. Moskalenko, S. Pensotti, T. A. Porter, L. Quadrani, P. G. Rancoita, D. Rozza, and M. Tacconi. HelMod in the Works: From Direct Observations to the Local Interstellar Spectrum of Cosmic-Ray Electrons. *ApJ*, 854:94, February 2018.
- [7] Cheng-Rui Zhu, Qiang Yuan, and Da-Ming Wei. Studies on Cosmic-Ray Nuclei with Voyager, ACE, and AMS-02. I. Local Interstellar Spectra and Solar Modulation. *ApJ*, 863:119, August 2018.

- [8] J. R. Jokipii. Radial Variation of Magnetic Fluctuations and the Cosmic-Ray Diffusion Tensor in the Solar Wind. *ApJ*, 182:585–600, June 1973.
- [9] A. Teufel and R. Schlickeiser. Analytic calculation of the parallel mean free path of heliospheric cosmic rays. I. Dynamical magnetic slab turbulence and random sweeping slab turbulence. *A&A*, 393:703–715, October 2002.
- [10] J. W. Bieber. Transport of charged particles in the heliosphere: Theory. *Advances in Space Research*, 32:549–560, August 2003.
- [11] J. W. Bieber, W. H. Matthaeus, A. Shalchi, and G. Qin. Nonlinear guiding center theory of perpendicular diffusion: General properties and comparison with observation. *Geophys. Res. Lett.*, 31:L10805, May 2004.
- [12] S. Parhi, J. W. Bieber, W. H. Matthaeus, and R. A. Burger. Heliospheric solar wind turbulence model with implications for ab initio modulation of cosmic rays. *Journal of Geophysical Research (Space Physics)*, 109:A01109, January 2004.
- [13] A. Shalchi, editor. *Nonlinear Cosmic Ray Diffusion Theories*, volume 362 of *Astrophysics and Space Science Library*, 2009.
- [14] C. Pei, J. W. Bieber, B. Breech, R. A. Burger, J. Clem, and W. H. Matthaeus. Cosmic ray diffusion tensor throughout the heliosphere. *Journal of Geophysical Research (Space Physics)*, 115:A03103, March 2010.
- [15] L. L. Zhao, L. Adhikari, G. P. Zank, Q. Hu, and X. S. Feng. Influence of the Solar Cycle on Turbulence Properties and Cosmic-Ray Diffusion. *ApJ*, 856:94, April 2018.
- [16] Z. N. Shen and G. Qin. Modulation of Galactic Cosmic Rays in the Inner Heliosphere over Solar Cycles. *ApJ*, 854:137, February 2018.
- [17] E. C. Stone, A. C. Cummings, F. B. McDonald, B. C. Heikkila, N. Lal, and W. R. Webber. Voyager 1 Observes Low-Energy Galactic Cosmic Rays in a Region Depleted of Heliospheric Ions. *Science*, 341:150–153, July 2013.

- [18] D. A. Gurnett, W. S. Kurth, L. F. Burlaga, and N. F. Ness. In Situ Observations of Interstellar Plasma with Voyager 1. *Science*, 341:1489–1492, September 2013.
- [19] A. C. Cummings, E. C. Stone, B. C. Heikkila, N. Lal, W. R. Weber, G. Jóhannesson, I. V. Moskalenko, E. Orlando, and T. A. Porter. Galactic Cosmic Rays in the Local Interstellar Medium: Voyager 1 Observations and Model Results. *ApJ*, 831:18, November 2016.
- [20] O. Adriani et al. Time Dependence of the Proton Flux Measured by PAMELA during the 2006 July-2009 December Solar Minimum. *ApJ*, 765:91, March 2013.
- [21] M. Martucci et al. Proton Fluxes Measured by the PAMELA Experiment from the Minimum to the Maximum Solar Activity for Solar Cycle 24. *ApJ*, 854:L2, February 2018.
- [22] M. S. Potgieter, E. E. Vos, M. Boezio, N. De Simone, V. Di Felice, and V. Formato. Modulation of Galactic Protons in the Heliosphere During the Unusual Solar Minimum of 2006 to 2009. *Sol. Phys.*, 289:391–406, January 2014.
- [23] Etienne E. Vos and Marius S. Potgieter. New Modeling of Galactic Proton Modulation during the Minimum of Solar Cycle 23/24. *ApJ*, 815(2):119, Dec 2015.
- [24] C. Corti, V. Bindi, C. Consolandi, and K. Whitman. Solar Modulation of the Local Interstellar Spectrum with Voyager 1, AMS-02, PAMELA, and BESS. *ApJ*, 829(1):8, Sep 2016.
- [25] J. L. Raath, M. S. Potgieter, R. D. Strauss, and A. Kopp. The effects of magnetic field modifications on the solar modulation of cosmic rays with a SDE-based model. *Advances in Space Research*, 57(9):1965–1977, May 2016.
- [26] N. Tomassetti, M. Orcinha, F. Barão, and B. Bertucci. Evidence for a Time Lag in Solar Modulation of Galactic Cosmic Rays. *ApJ*, 849:L32, November 2017.
- [27] G. Qin and Z.-N. Shen. Modulation of Galactic Cosmic Rays in the Inner Heliosphere, Comparing with PAMELA Measurements. *ApJ*, 846:56, September 2017.



- [28] M. Aguilar et al. Observation of Fine Time Structures in the Cosmic Proton and Helium Fluxes with the Alpha Magnetic Spectrometer on the International Space Station. *Phys. Rev. Lett.*, 121(5):051101, 2018.
- [29] N. Tomassetti, F. Barão, B. Bertucci, E. Fiandrini, J. L. Figueiredo, J. B. Lousada, and M. Orcinha. Testing Diffusion of Cosmic Rays in the Heliosphere with Proton and Helium Data from AMS. *Physical Review Letters*, 121(25):251104, December 2018.
- [30] C. Corti, M. S. Potgieter, V. Bindi, C. Consolandi, C. Light, M. Palermo, and A. Popkow. Numerical Modeling of Galactic Cosmic-Ray Proton and Helium Observed by AMS-02 during the Solar Maximum of Solar Cycle 24. *ApJ*, 871:253, February 2019.
- [31] Bing-Bing Wang, Xiao-Jun Bi, Kun Fang, Su-Jie Lin, and Peng-Fei Yin. Time-dependent solar modulation of cosmic rays from solar minimum to solar maximum. *Phys. Rev. D*, 100(6):063006, Sep 2019.
- [32] R. Kappl. SOLARPROP: Charge-sign dependent solar modulation for everyone. *Computer Physics Communications*, 207:386–399, October 2016.
- [33] E. N. Parker. The passage of energetic charged particles through interplanetary space. *Planetary and Space Science*, 13:9–49, January 1965.
- [34] L. J. Gleeson and I. H. Urch. Energy losses and modulation of galactic cosmic rays. *Ap&SS*, 11:288–308, May 1971.
- [35] L. A. Fisk. Solar modulation of galactic cosmic rays, 2. *J. Geophys. Res.*, 76:221, 1971.
- [36] G. J. Fulks. Solar modulation of galactic cosmic ray electrons, protons, and alphas. *J. Geophys. Res.*, 80:1701–1714, May 1975.
- [37] H. Moraal. Cosmic-Ray Modulation Equations. *Space Sci. Rev.*, 176:299–319, June 2013.
- [38] M. J. Boschini, S. Della Torre, M. Gervasi, G. La Vacca, and P. G. Rancoita. Propagation of cosmic rays in heliosphere: The HELMOD model. *Advances in Space Research*, 62:2859–2879, November 2018.
- [39] A. Vittino, C. Evoli, and D. Gaggero. Cosmic-ray transport in the heliosphere with HELIOPROP. *International Cosmic Ray Conference*, 35:24, January 2017.

- [40] E. N. Parker. Dynamics of the Interplanetary Gas and Magnetic Fields. *ApJ*, 128:664, November 1958.
- [41] J. Giacalone and J. R. Jokipii. The Transport of Cosmic Rays across a Turbulent Magnetic Field. *ApJ*, 520:204–214, July 1999.
- [42] J. R. Jokipii, E. H. Levy, and W. B. Hubbard. Effects of particle drift on cosmic-ray transport. I - General properties, application to solar modulation. *ApJ*, 213:861–868, May 1977.
- [43] R. A. Burger and M. S. Potgieter. The calculation of neutral sheet drift in two-dimensional cosmic-ray modulation models. *ApJ*, 339:501–511, April 1989.
- [44] S. E. S. Ferreira, M. S. Potgieter, and B. Heber. Particle drift effects on cosmic ray modulation during solar maximum. *Advances in Space Research*, 32:645–650, August 2003.
- [45] M. S. Potgieter, E. E. Vos, R. Munini, M. Boezio, and V. Di Felice. Modulation of Galactic Electrons in the Heliosphere during the Unusual Solar Minimum of 2006-2009: A Modeling Approach. *ApJ*, 810:141, September 2015.
- [46] M. S. Potgieter, J. A. Le Roux, L. F. Burlaga, and F. B. McDonald. The role of merged interaction regions and drafts in the heliospheric modulation of cosmic rays beyond 20 AU - A computer simulation. *ApJ*, 403:760–768, February 1993.
- [47] M. S. Potgieter. Time-dependent cosmic-ray modulation - Role of drifts and interaction regions. *Advances in Space Research*, 13:239–249, June 1993.
- [48] Xi Luo, Marius S. Potgieter, Veronica Bindi, Ming Zhang, and Xue-shang Feng. A Numerical Study of Cosmic Proton Modulation Using AMS-02 Observations. *ApJ*, 878(1):6, Jun 2019.
- [49] A. Ghelfi, F. Barao, L. Derome, and D. Maurin. Non-parametric determination of H and He interstellar fluxes from cosmic-ray data. *A&A*, 591:A94, June 2016.
- [50] N. Gopalswamy, A. Lara, S. Yashiro, and R. A. Howard. Coronal Mass Ejections and Solar Polarity Reversal. *ApJ*, 598:L63–L66, November 2003.

- [51] N. Karna, S. A. Hess Webber, and W. D. Pesnell. Using Polar Coronal Hole Area Measurements to Determine the Solar Polar Magnetic Field Reversal in Solar Cycle 24. *Sol. Phys.*, 289:3381–3390, September 2014.
- [52] X. Sun, J. T. Hoeksema, Y. Liu, and J. Zhao. On Polar Magnetic Field Reversal and Surface Flux Transport During Solar Cycle 24. *ApJ*, 798:114, January 2015.
- [53] A. G. Tlatov, D. V. Dormidontov, R. V. Kirpichev, M. P. Pashchenko, A. D. Shramko, V. S. Peshcherov, V. M. Grigoryev, M. L. Demidov, and P. M. Svidskii. Study of some characteristics of large-scale solar magnetic fields during the global field polarity reversal according to observations at the telescope-magnetograph Kislovodsk Observatory. *Geomagnetism and Aeronomy*, 55:969–975, December 2015.
- [54] M. I. Pishkalo and U. M. Leiko. Dynamics of the circumpolar magnetic field of the Sun at a maximum of cycle 24. *Kinematics and Physics of Celestial Bodies*, 32:78–85, March 2016.
- [55] N. Gopalswamy, S. Yashiro, and S. Akiyama. Unusual Polar Conditions in Solar Cycle 24 and Their Implications for Cycle 25. *ApJ*, 823:L15, May 2016.
- [56] P. Janardhan, K. Fujiki, M. Ingale, S. K. Bisoi, and D. Rout. Solar cycle 24: An unusual polar field reversal. *A&A*, 618:A148, October 2018.
- [57] A. Ghelfi, D. Maurin, A. Cheminet, L. Derome, G. Hubert, and F. Melot. Neutron monitors and muon detectors for solar modulation studies: 2.  $\phi$  time series. *Advances in Space Research*, 60:833–847, August 2017.
- [58] Sergey A. Koldobskiy, Veronica Bindi, Claudio Corti, Gennady A. Kovaltsov, and Ilya G. Usoskin. Validation of the Neutron Monitor Yield Function Using Data From AMS-02 Experiment, 2011-2017. *Journal of Geophysical Research (Space Physics)*, 124(4):2367–2379, Apr 2019.
- [59] J. Minnie, J. W. Bieber, W. H. Matthaeus, and R. A. Burger. Suppression of Particle Drifts by Turbulence. *ApJ*, 670:1149–1158, December 2007.
- [60] N. Marcelli, O. Adriani, G. C. Barbarino, G. A. Bazilevskaya, R. Bellotti, M. Boezio, E. A. Bogomolov, M. Bonggi, V. Bonvicini, and S. Bottai. Time dependence of the helium flux measured by PAMELA. In

*European Physical Journal Web of Conferences*, volume 209 of *European Physical Journal Web of Conferences*, page 01004, Sep 2019.

## A The comparison of LIS in Paper I

In the Paper I, the proton (helium) LIS is based on the Voyager 1 and PAMELA (BESS-POLARII) data. We show the comparison of LIS obtained in this work and these in the Paper I at the top panel of Figure 6. In the bottom panel, we show the ratio of LIS relative to these in the Paper I. The differences of the LIS are no more than 5%.

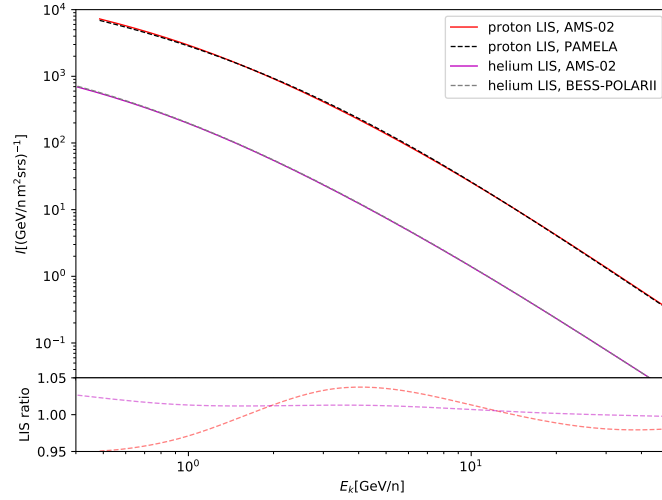


Figure 6: The comparison of LIS of proton and helium from the Paper I and this work.

## B Full drift in the positive polarity cycle

Under the assumption of the positive polarity and the full drift effect, the time profile of  $k_0$  is shown in Figure 7. The difference of  $\chi^2$  between the full drift and the suppressed drift scenario are also shown. The full drift scenario leads to very small  $k_0$  and larger  $\chi^2$ .

## C The degeneracy between $k_0$ and $k_d$

One example of the degeneracy between the diffusion and the drift is shown in Figure 8. The computed spectra is compared to the proton data

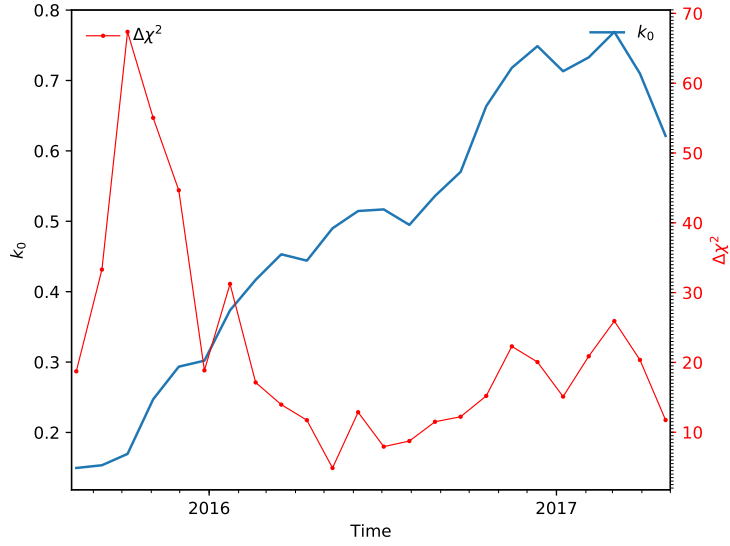


Figure 7: The time profile of  $k_0$  with the assumption of the positive polarity and the full drift. The  $\chi^2$  difference between the full drift scenario and the suppressed drift scenario is marked as  $\Delta\chi^2$ .

taken during 2017/04/13 to 2017/05/09.  $k_0$  and  $k_d$  are taken as model input parameters and  $\chi^2$  values are computed on the grid. It can be seen that, there is a obvious degeneracy between  $k_0$  and  $k_d$ . Since the drift effect are opposite for proton and antiproton, the future monthly antiproton data from AMS-02 is critical to break the degeneracy and improve our understanding on the modulation process.

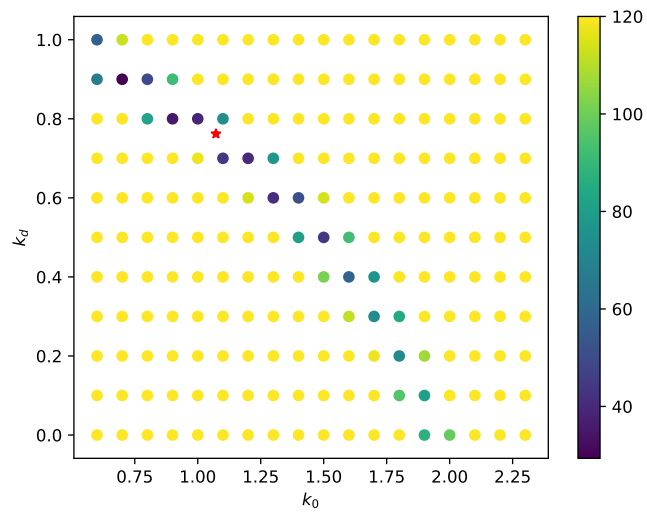


Figure 8: The degeneracy between  $k_0$  and  $k_d$ . The red star indicates the best fit value. The color indicates the  $\chi^2$  value in the grid.